Original Article

Identification of the function of *FOSB* in cholangiocarcinoma using bioinformatics analysis

Yihang Zhao^, Hong Tang, Yaxian Kuai, Jianhua Xu, Bin Sun, Yang Li

Department of Gastroenterology, The First Affiliated Hospital of Anhui Medical University, Hefei, China

Contributions: (I) Conception and design: Y Li; (II) Administrative support: Y Li; (III) Provision of study materials or patients: H Tang, J Xu; (IV) Collection and assembly of data: B Sun, Y Kuai; (V) Data analysis and interpretation: Y Zhao; (VI) Manuscript writing: All authors; (VII) Final approval of manuscript: All authors.

Correspondence to: Yang Li, MD, PhD. Department of Gastroenterology, The First Affiliated Hospital of Anhui Medical University, 218 Jixi Road, Hefei, China. Email: bladehall@163.com.

Background: Exploring the potential mechanism of cholangiocarcinoma (CCA) metabolic reprogramming is significant for guiding clinical treatment. However, related research and exploration are still lacking. Therefore, we aimed to identify a reliable metabolism-related gene or biomarker of CCA using bioinformatics analysis.

Methods: The GSE26566, GSE45001, and GSE132305 datasets were obtained from the Gene Expression Omnibus (GEO) database. Differently expressed genes (DEGs) between CCA tissues and adjacent tissues were screened out. The key gene was identified through enrichment and functional analysis, and its immune and clinical correlation was investigated utilizing the Tumor Immune Evaluation Resource (TIMER2.0), the Tumor-Immune System Interactions Database (TISIDB), the Gene Expression Profiling Interactive Analysis (GEPIA2), and the Kaplan-Meier Plotter. Finally, immunohistochemistry (IHC) was performed to validate the results.

Results: By analysis, the expression of FBJ murine osteosarcoma viral oncogene homolog B (*FOSB*) was significantly downregulated in CCA tissues when compared with adjacent tissues. Moreover, the expression levels of *FOSB* positively correlated with tumor-infiltrating immune cells in most tumors, and patients with high *FOSB* expression tended to have a better prognosis. The *FOSB* and *SIRT3/HIF1A* axes have similar expression trends and metabolic functions in CCA cells, and the correlation between of them was preliminarily explored by IHC experiments.

Conclusions: The expression levels of *FOSB* are closely related to the prognosis of CCA patients, which may be a predictive indicator for prognosis and immunotherapy.

Keywords: Cholangiocarcinoma (CCA); *FOSB*; immune infiltration; pancancer analysis; *SIRT3*

Submitted May 15, 2023. Accepted for publication Sep 28, 2023. Published online Dec 01, 2023.
doi: 10.21037/tcr-23-829
View this article at: https://dx.doi.org/10.21037/tcr-23-829

Introduction

As a malignant tumor with low incidence but high mortality, cholangiocarcinoma (CCA) can be divided into three subtypes according to its origin: intrahepatic CCA (iCCA), periportal CCA (pCCA), and distal CCA (dCCA) (1). It is characterized by occult presentation in the early stage, high malignancy in the late stage, poor prognosis, and a distinct geographical distribution (2,3). In recent years, the incidence of CCA has been rising, indicating that more attention must be paid to the prevention and treatment

^ ORCID: 0000-0002-1437-5933.

of CCA. Surgery is still the primary clinical treatment, supplemented by radiotherapy and chemotherapy (4-7). However, due to the limitations of surgical treatment and the high recurrent rate of CCA, the 5-year survival rates of patients have been extremely low (6,8,9). Therefore, there is an urgent need to explore its underlying molecule mechanisms.

Numerous studies have demonstrated that the progress of malignant tumors is closely related to metabolic reprogramming (10). Among CCA cell lines, those with greater uptake and oxidation capacity of fatty acid (FA) have tended to be more aggressive (10-12). Moreover, the lipid metabolism-related prostaglandins (PG) and the enzyme sphingosine kinase (SPHK) have also been verified to be correlated with the malignant phenotype (13-15). In addition, the progress of CCA has been shown to be closely related to glucose metabolism (16). Previous studies have found that sirtuin 3 (*SIRT3*), a member of the deacetylase family, plays an important role in cancer metabolism and it is more typical in CCA. For example, *SIRT3* can influence the Warburg effect in tumor tissue by regulating the metabolism of key enzymes of the glycolytic pathway mediated by hypoxia-inducible factor A (*HIF1A*), which ultimately influences the establishment of the CCA cell phenotype (17).

FBJ murine osteosarcoma viral oncogene homolog B (*FOSB*), as a member of the Fos family, can regulate normal cellular physiological activities (18). However, its effect on the metabolic changes of cancer cells is still a mystery. It has been found that the members of the Fos protein family can promote the development and invasion of tumors by dimerizing with JUN proteins to form activator protein-1 (AP-1). The Hippo pathway Yes-associated protein (YAP) and AP-1 can synergistically promote the development of pancreatic and breast cancers (19-23). The cystathionine-β-synthase-hydrogen sulfide (CBS-H2S) axis can promote liver metastasis of colon cancer through AP-1 (24). Rac GTPase-activating protein 1 (RacGAP1) indirectly regulates AP-1 to induce the occurrence of cervical cancer. However, *FOSB* also seems to play a beneficial role, as it has been shown that in gastric cancer, when FOSB was overexpressed, the growth of tumor cells was significantly inhibited (25). In acute myeloid leukemia, patients with high *FOSB* expression tend to have a better prognosis (26). However, the potential role of *FOSB* in CCA remains unclear, and its potential molecular mechanism needs to be further explored. We present this article in accordance with the REMARK reporting checklist (available at https://tcr.amegroups.com/article/view/10.21037/tcr-23-829/rc).

Highlight box

Key findings

- Downregulation of *FOSB* expression is associated with poor prognosis of cholangiocarcinoma (CCA) and may act through regulation of related metabolic pathways.

What is known and what is new?

- The *SIRT3/HIF1A* axis affects CCA progression by regulating metabolism.
- We investigated the potential functional role of *FOSB* in CCA using bioinformatics analysis and preliminarily explored the association of this gene with the *SIRT3/HIF1A* axis.

What is the implication, and what should change now?

- Our study found the potential relationship between *FOSB* and CCA, which is of great significance for predicting the prognosis of CCA patients.

Methods

Acquisition of clinical samples

All samples (including 24 pairs of CCA and the corresponding adjacent tissues) were obtained from patients who were pathologically diagnosed with CCA at the First Affiliated Hospital of Anhui Medical University. Tissues were embedded with paraffin wax and stored under suitable conditions. The study was conducted in accordance with the Declaration of Helsinki (as revised in 2013). The study was approved by the Ethics Committee of Anhui Medical University (No. 20190199), and informed consent was provided by all patients.

Datasets downloading and differential analysis

The datasets (GSE26566, GSE45001, GSE132305) were downloaded from the Gene Expression Omnibus (GEO) database (https://www.ncbi.nlm.nih.gov/) and samples were divided into two groups as per the type of tissue: CCA and adjacent tissues. The data were normalized using the limma package of RStudio (Posit; Boston, MA, USA) and differently expressed genes (DEGs) were obtained between CCA and adjacent tissues [|log fold change (FC)| >1, P value <0.05, and the base of |logFC| was 2]. Then, the Venn diagram template from Bioinformatics & Evolutionary Genomics (http:// bioinformatics.psb.ugent.be/webtools/Venn/) was used to obtain the intersection

graph of the different groups of DEGs.

Protein-protein interaction network analysis

The online website (https://cn.string-db.org/cgi/input?sessionId=bEVgLvYZrtTp&input_page_active_form=multiple_sequences) was used for protein functional interaction analysis of the screened DEGs, and closely linked gene sets were further screened out by using the MCODE tool in Cytoscape software (https://cytoscape.org/) (27).

Enrichment analysis

The enrichment analysis and Gene Ontology (GO) enrichment picture were accomplished by the Enrichplot, clusterProfiler, and other toolkits of RStudio. Gene set enrichment analysis (GSEA) was conducted using limma, org.Hs.eg.db, clusterProfiler, enrich plot, and other installation packages of RStudio.

Survival analysis

Kaplan-Meier Plotter and Gene Expression Profiling Interactive Analysis (GEPIA2) website were used to plot the survival analysis map of tumors (28,29). The patients were divided into two groups, high- and low-expression groups, with the median as the group cutoff, and then the 95% confidence interval (CI) as the dotted line. Subsequently, CCA datasets were selected to plot the correlation curves ($P<0.05$ was considered statistically significant).

Pancancer and immune analysis

The Cancer Exploration panel of Tumor Immune Evaluation Resource (TIMER2.0; http://timer.cistrome.org/) was used to map the pancancer analysis (including 33 cancers) of *FOSB*. Data were collected from The Cancer Genome Atlas (TCGA) database, which contained 33 types of tumors, and all parameters were default values. Distributions of gene expression levels were displayed using box plots. The statistical significance computed by the Wilcoxon test is annotated by the number of asterisks (*, $P<0.05$; **, $P<0.01$; ***, $P<0.001$). The Tumor-Immune System Interactions Database (TISIDB) online platform (http://cis.hku.hk/TISIDB/) was applied to analyze the correlation between *FOSB* and tumor-infiltrating immune cells and immune-related factors in tumors ($P<0.05$ was considered statistically significant) (30,31).

GSEA

Limma, org.Hs.eg.db, clusterProfiler, enrichplot, and other installation packages of RStudio were used to divide the screened key genes into high- and low-expression groups and plot the functional enrichment analysis was used to identify the key gene.

Immunohistochemistry (IHC)

The embedded tissues were cut into 4 μm sections. Dewaxing and hydration were performed in xylene and fractionated ethanol. Endogenous peroxidase blocking solution was added dropwise to inhibit the endogenous peroxidase activity of the tissue, and then ethylenediaminetetraacetic acid (EDTA) repair solution (BL618A, Biosharp, Hefei, China) was used for antigen repair. After being blocked with normal serum solution, sections were incubated with antibodies of SIRT3 (s4072; Sigma-Aldrich, St. Louis, MO, USA), HIF1α [36169; Cell Signaling Technology (CST), Danvers, MA, USA], and *FOSB* (ab184938; Abcam, Cambridge, UK) overnight. Then, the goat anti-rabbit IgG secondary antibody (1:4,000–80,000, BL003A, Biosharp) coupled with horseradish peroxidase (HRP) was added. Finally, the slices were stained with diaminobenzidine (DAB) chromogenic solution (BL732A, Biosharp) and hematoxylin staining solution and dehydrated using fractionated ethanol and xylene. Finally, the slices were sealed with neutral gum and observed under a light microscope. The grading of staining intensity was as follows: absent staining =0, weak =1, moderate =2, and strong =3. The percentage of staining was graded as follows: 0 (no positive cells), 1 (<25% positive cells), 2 (25–50% positive cells), 3 (>50–75% positive cells), and 4 (>75% positive cells). The score for each tissue was calculated by multiplication; the range of this calculation was therefore 0 to 12.

Statistical analysis

The software SPSS 23.0 (IBM Corp., Armonk, NY, USA) was used for statistical analysis in this study and Student's *t*-test was used to analysis the statistical differences among experimental groups. Statistical significance was considered when $P<0.05$.

Results

Screening of DEGs

Firstly, DEGs were screened from all datasets (|logFC|

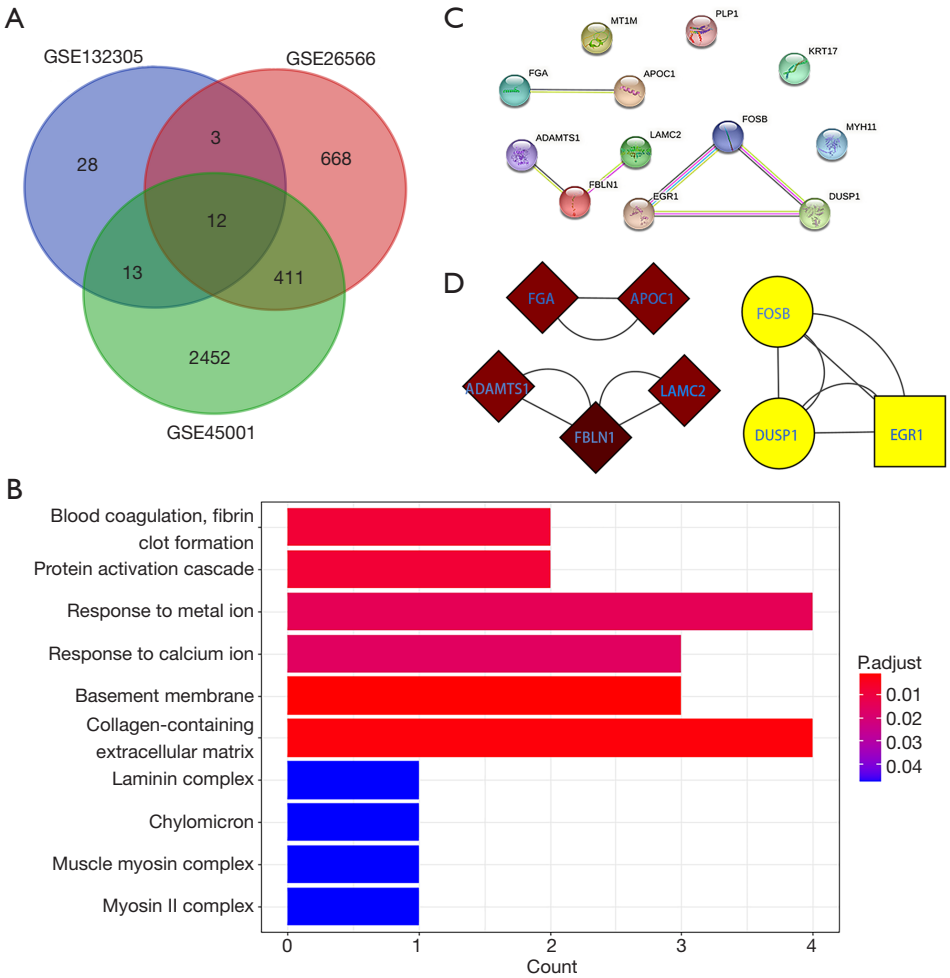

Figure 1 Screening of key genes. (A) Venn diagram of DEGs in three data sets. (B) Functional enrichment analysis. (C) PPI network analysis. (D) The three gene sets screened by MCODE (a tool for analyzing gene enrichment degrees in Cytoscape software). DEGs, differently expressed genes; PPI, protein-protein interaction.

>1, P<0.05), in which 1,094 DEGs were obtained from GSE26566, 2,888 DEGs from GSE45001, and 56 DEGs from GSE132305. Then, we mapped the Venn diagram to find the intersection of all screened DEGs (*Figure 1A*) and finally obtained 12 DEGs between CCA and adjacent tissues (*FOSB*, *DUSP1*, *EGR1*, *FGA*, *APOC1*, *ADAMTS1*, *FBLN1*, *LAMC2*, *KRT17*, *PLP1*, *MT1M*, *MYH11*). Moreover, we performed functional enrichment analysis for these DEGs and found that these genes were most closely related to the functions of blood coagulation, response to metal ion, basement membrane, and collagen-containing extracellular matrix (*Figure 1B*). We finally screened out the key gene *FOSB* by combining the results of the above analysis. In addition, protein-protein interaction (PPI) analysis (*Figure 1C*) and the MCODE tool in Cytoscape were used to obtain the most enriched gene set (*Figure 1D*). The results showed that *FOSB*, *DUSP1*, and *EGR1* had the highest enrichment score, and *FOSB* was in the core position. Therefore, combined with the above analysis, we finally screened out the key gene *FOSB*.

Expression analysis

We performed further expression analysis on the screened key genes. Firstly, the pan-cancer analysis of *FOSB* was carried out by using the pan-cancer analysis module of TIMER2.0 (*Figure 2A*) to observe the overall differential expression in malignant tissues and normal tissues. Moreover, Rstudio ranked its expression levels in these tumors (*Figure 2B*). The results revealed that the expression

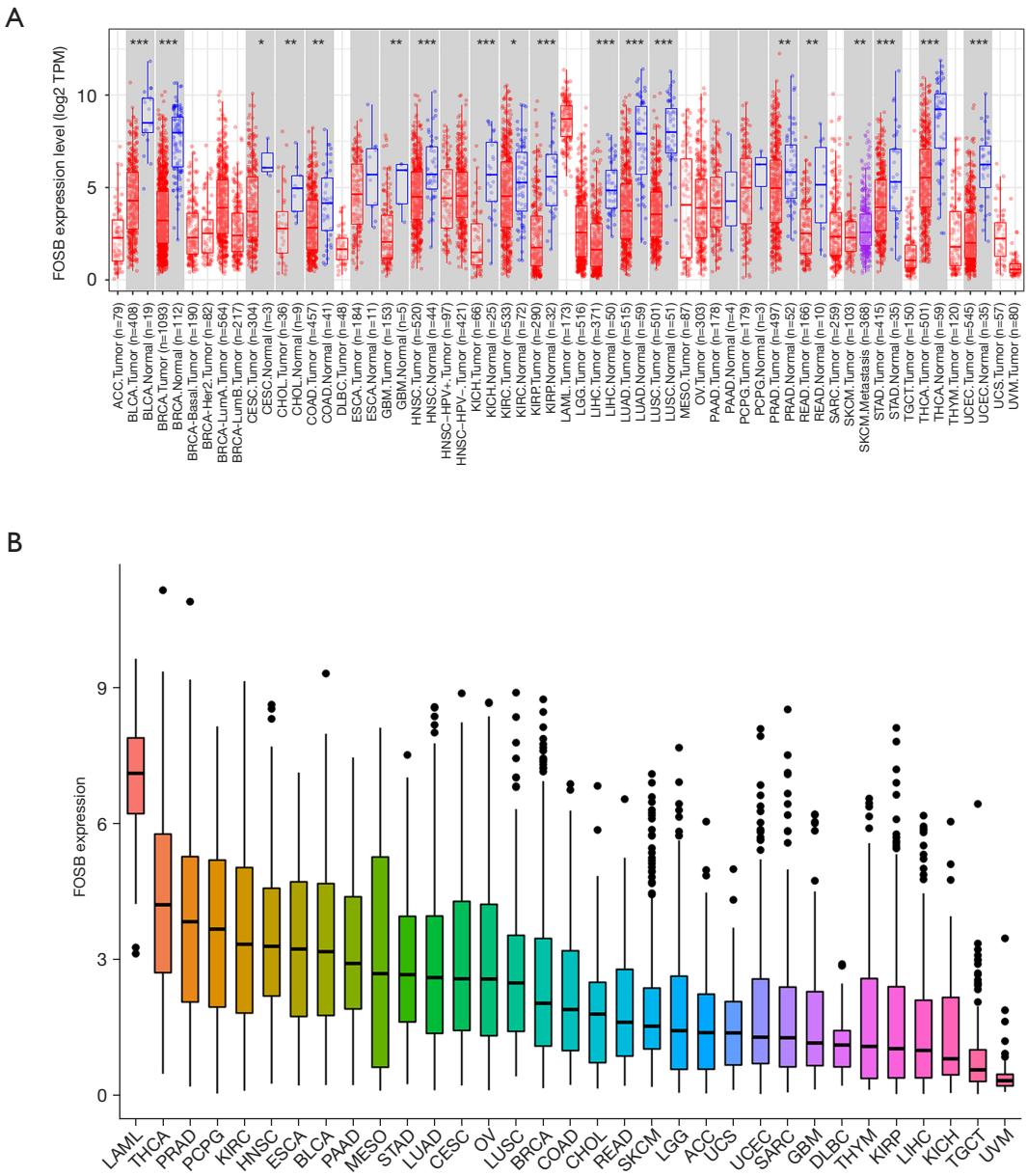

Figure 2 Pancancer analysis of *FOSB*. (A) Differences in the expression levels of *FOSB* between various malignant tumors and corresponding paraneoplastic tissues. The statistical significance computed by the Wilcoxon test is annotated by the number of stars (red and blue are tumors and normal tissues, respectively; *, P<0.05; **, P<0.01; ***, P<0.001). (B) Differences in the expression levels of *FOSB* in various malignant tumors. TPM, transcripts per million; *FOSB*, FBJ murine osteosarcoma viral oncogene homolog B.

levels of *FOSB* were downregulated in CCA and most malignant tumors.

FOSB clinical correlation analysis

Based on the analysis of the differences in *FOSB* expression, we further analyzed the differences in *FOSB* activity levels in various malignancies (*Figure 3A*). We plotted a gradient box plot from high to low according to the activity levels (*Figure 3B*), which was used to visualize the overall activity of *FOSB* in various cancers. The results showed that the *FOSB* activity levels in CCA were significantly reduced.

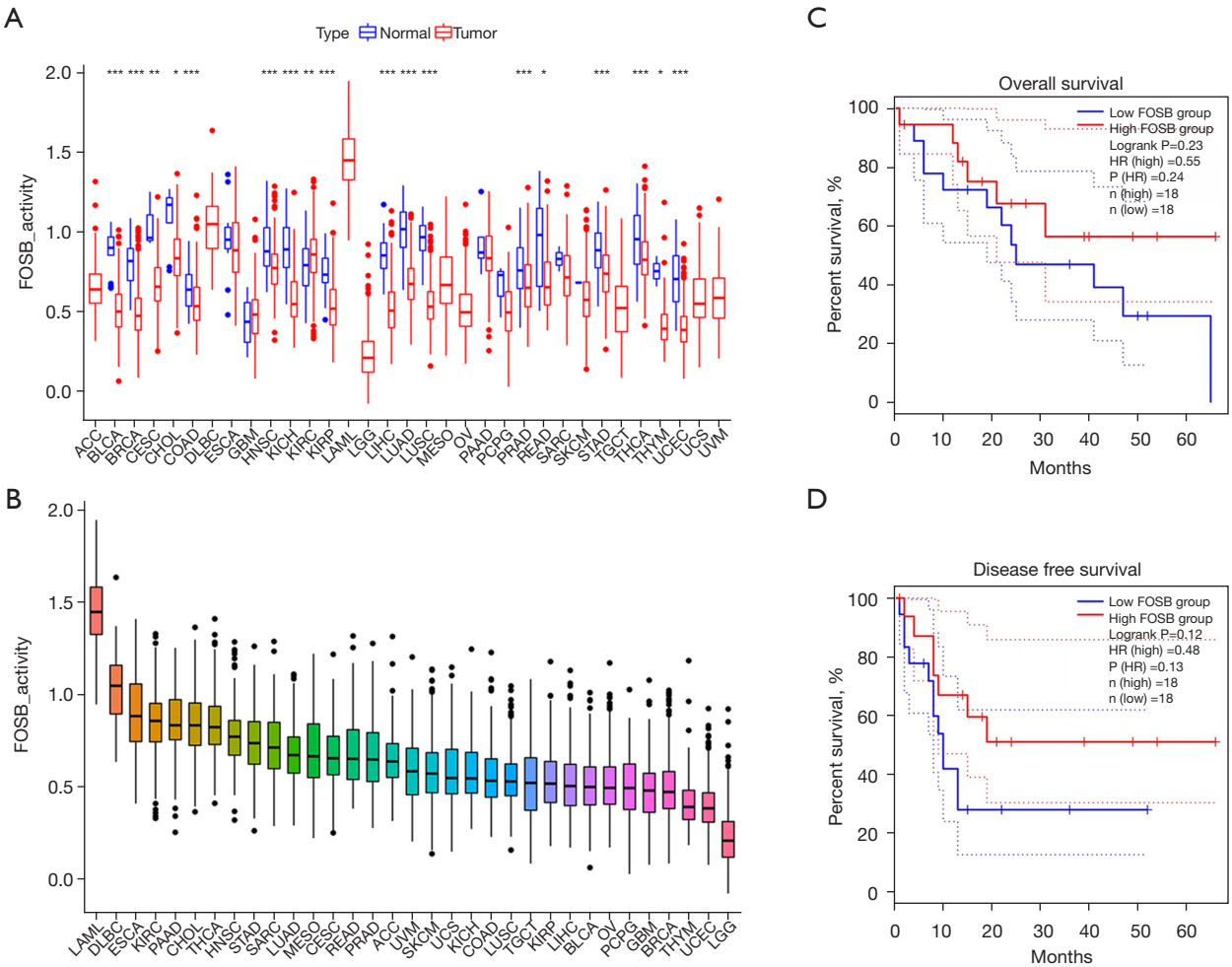

Figure 3 Clinical correlation analysis of *FOSB*. (A) Differences in gene activity of *FOSB* in various malignancies and corresponding paraneoplastic tissues (*, P<0.05; **, P<0.01; ***, P<0.001). (B) Gradient analysis of the gene activity levels of *FOSB* in various tumors. (C,D) Overall survival and disease-free survival were analyzed for CCA patients. According to the expression level of *FOSB*, the patients were divided into two cohorts on average: high-expression group and low-expression group. The cutoff value was as follows: P<0.01 and |logFC| >1. *FOSB*, FBJ murine osteosarcoma viral oncogene homolog B; CCA, cholangiocarcinoma; FC, fold change.

Kaplan-Meier Plotter and GEPIA2 websites were used to plot survival analyses curves of different cancers. Patients were evenly divided into high- and low-expression groups. The results showed that kidney and lung cancer patients with high levels of *FOSB* tend to have a better prognosis (Figure S1), and the same trend could be observed in CCA patients. However, because of the limited sample size of CCA, no significant difference could be seen for the time being (*Figure 3C,3D*)

The correlation analysis of tumor-infiltrating immune cells

To further investigate the role played by *FOSB* in CCA, we used TIMER2.0 to analyze the correlation between *FOSB* expression and tumor-infiltrating immune cells in tumors based on different algorithms. We found that *FOSB* showed a similar trend with tumor-infiltrating immune cells in most malignancies. Especially in CCA, *FOSB* showed a high positive correlation with macrophage, monocyte,

cancer-associated fibroblasts (CAFs), endothelial cells, hematopoietic stem cells, mast cells, T cell follicular helper, $CD4^+$, and other tumor-infiltrating immune cells (*Figure 4A*), and we obtained similar results with the analysis on TISIDB (*Figure 4B*). Moreover, *FOSB* was significantly associated with immune activators, immunosuppressive factors, and MH4C molecules, and the same was observed in hepatocellular carcinoma (*Figure 4C-4E*). These data demonstrated that *FOSB* is largely involved in the tumor-infiltrating immune cells in tumors and plays an important role in tumor immunity, which may also be related to the fact that patients with high *FOSB* expression tend to have a better prognosis. The above information demonstrates the potential impact of *FOSB* on tumor-infiltrating immune cells in the tumor microenvironment (TME) of CCA.

GSEA

GSEA of *FOSB* was conducted to find the core pathways that may play a significant role in CCA, and the diagram was drawn through Rstudio and its installation package. The results showed that in CCA, the group with high expression levels of *FOSB* was mainly enriched in arachidonic acid metabolism, cell adhesion molecules (CAMs), glutathione metabolism, glycerol metabolism, hypertrophic cardiomyopathy, and other pathways (*Figure 5*). Previous studies have found that metabolic pathways play a critical role in the regulation of CCA (17). Therefore, we speculated that *FOSB* would also play a vital role in CCA metabolism.

Role of SIRT3/HIF1A/FOSB in CCA

In our previous study, we discovered the interaction between *SIRT3* and *HIF1A* in CCA and that they play an important role in influencing the metabolic process of the tumor cells (17). These findings coincide with our prediction of the role of *FOSB* in metabolism. Our analysis found an obvious association between *FOSB* expression trends and the *SIRT3/HIF1A* axis. The potential association between *FOSB* and *HIF1A* has also been uncovered in other studies (32,33). To test our conjecture, we conducted the corresponding IHC and analyzed the obtained CCA and corresponding paraneoplastic tissues. The results showed that the expression levels of *SIRT3* and *FOSB* were significantly decreased in CCA, whereas the expression of *HIF1A* was significantly increased (*Figure 6*). Therefore, we preliminarily assume that *FOSB* acts downstream of the *SIRT3/HIF1A* axis.

Discussion

We analyzed all datasets (GSE26566, GSE45001, and GSE132305) obtained from the GEO database and obtained the DEGs between CCA and adjacent tissues. Then, *FOSB* was screened out using PPI analysis and enrichment analysis. Compared to normal tissues, the expression levels of *FOSB* in malignant tumors were significantly decreased. To explore the potential role of *FOSB* in CCA, we analyzed the influence of *FOSB* on the survival rate of all cancer patients using the Kaplan-Meier plotter. The results showed that CCA patients with high expression of the *FOSB* gene tend to have a better prognosis. Therefore, we speculated that *FOSB* could play an important role in inhibiting the progress of tumors.

To further test our hypothesis, the TIMER2.0 website was used to explore the association between *FOSB* and tumor-infiltrating immune cells. The results showed that *FOSB* was positively related to most tumor-infiltrating immune cells. Interestingly, we discovered that there was a significant positive correlation between *FOSB* and CAFs, which was an indispensable part of the TME (34). Many studies have shown that CAFs may have both cancer-promoting and cancer-suppressing effects. For example, in pancreatic ductal adenocarcinoma (PDAC), CAFs can promote tumor invasion, whereas their depletion can lead to tumor progression (35-37). Although many studies have explored the cancer-promoting effects of CAFs in CCA, such as inhibition of apoptosis, promotion of migration and invasion, and so on, they have been identified as a meaningful target for the treatment and prevention of CCA (38-41). However, given the lack of functional studies and the limitations of the size of clinical trials, we still cannot conclude that there are other roles for CAFs in CCA, and it would be interesting to know whether there are other roles for CAFs in CCA.

The relationship between *SIRT3* and *HIF1A* in CCA was discussed in the preliminary study. The results showed that when SIRT3 was overexpressed, the production of reactive oxygen species (ROS) decreased significantly under hypoxia. Therefore, the instability of *HIF1A* would increase and inhibit the development of tumors (42). In recent years, many studies have explored the role of the *SIRT3/HIF1A* axis in substance metabolism. For example, knocking down *SIRT3* in Newcastle disease virus (NDV)-infected cells was shown to help maintain the stability of *HIF1A* and

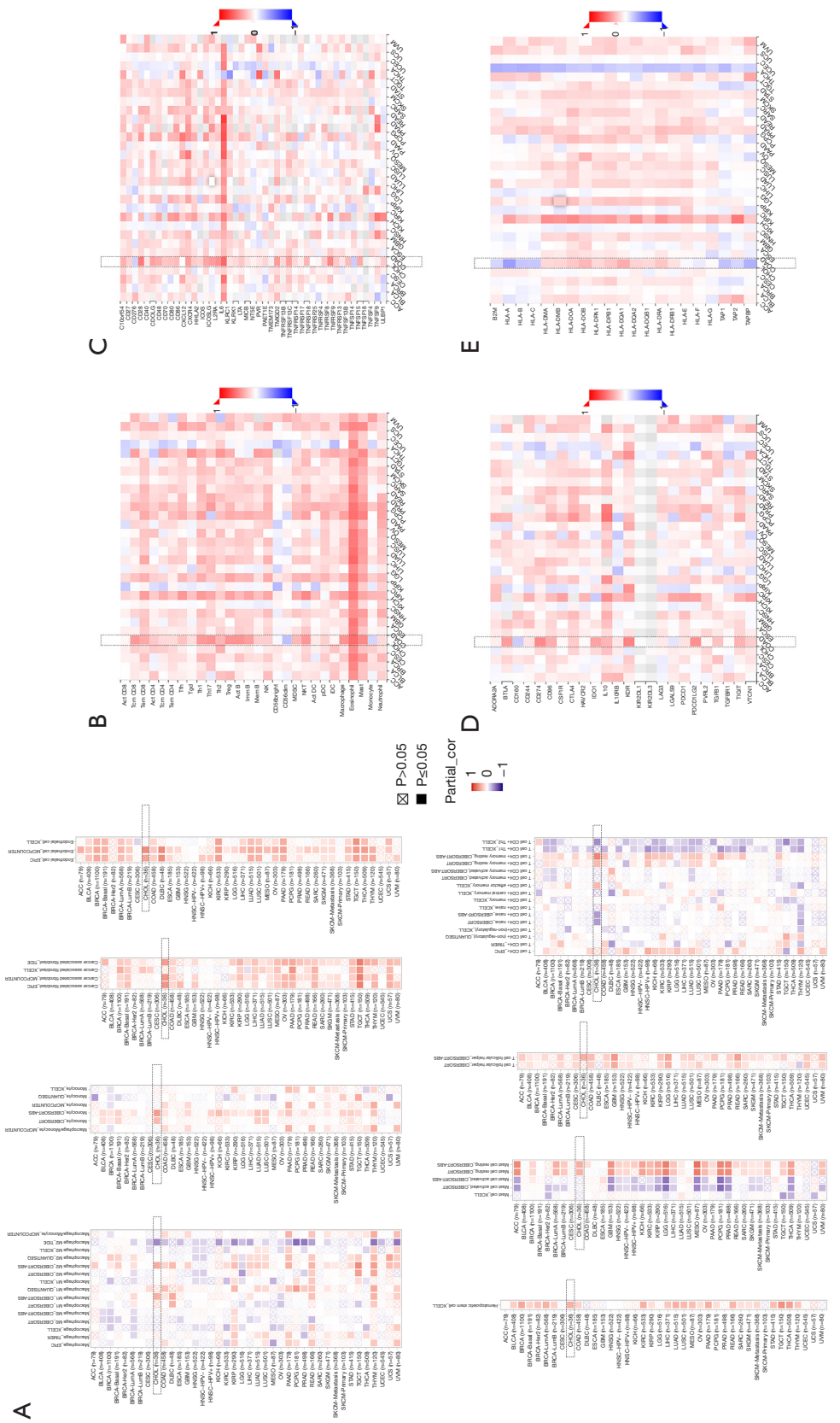

Figure 4 Immunological analysis of *FOSB* associated with tumors. (A,B) Correlation analysis of *FOSB* expression with tumor-infiltrating immune cells (red represents positive correlation, blue represents negative correlation). (C-E) Correlation analysis of *FOSB* expression with immune-suppressive factors, immune-activating factors, and major histocompatibility complexes molecules (red represents positive correlation, blue represents negative correlation). *FOSB*, FBJ murine osteosarcoma viral oncogene homolog B.

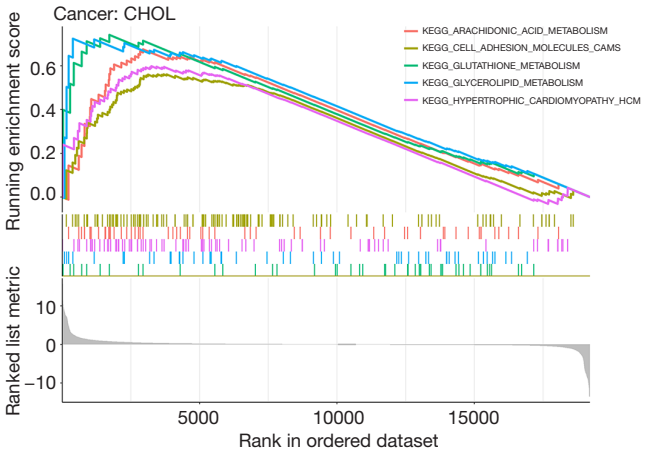

Figure 5 GSEA of *FOSB* in CCA. GSEA, gene set enrichment analysis; *FOSB*, FBJ murine osteosarcoma viral oncogene homolog B; CCA, cholangiocarcinoma; KEGG, Kyoto Encyclopedia of Genes and Genomes.

ultimately affect the glycolytic process and promote viral replication (43). In addition, the *SIRT3/HIF1A* axis has been shown to alter tumor development by affecting the activity of key enzymes of the glycolytic pathway and subsequently the Warburg effect (17,44). Given the strong similarity between *FOSB* and *HIF1A* in terms of metabolism and altered physiological activity under hypoxia, we speculate that *HIF1A* and *FOSB* may have a potential link (45-47). Subsequently, we performed IHC experiments using the collected CCA tissues and found that *SIRT3/HIF1A* may influence the malignant phenotype of CCA by regulating *FOSB* and then regulating other metabolic pathways. However, whether its function is based on the *SIRT3/HIF1A* axis is worthy of further investigation.

There are still many mysteries and disputes about the role of *FOSB* in cancer. Although it may function as a cancer promoter in malignant tumors such as prostate cancer,

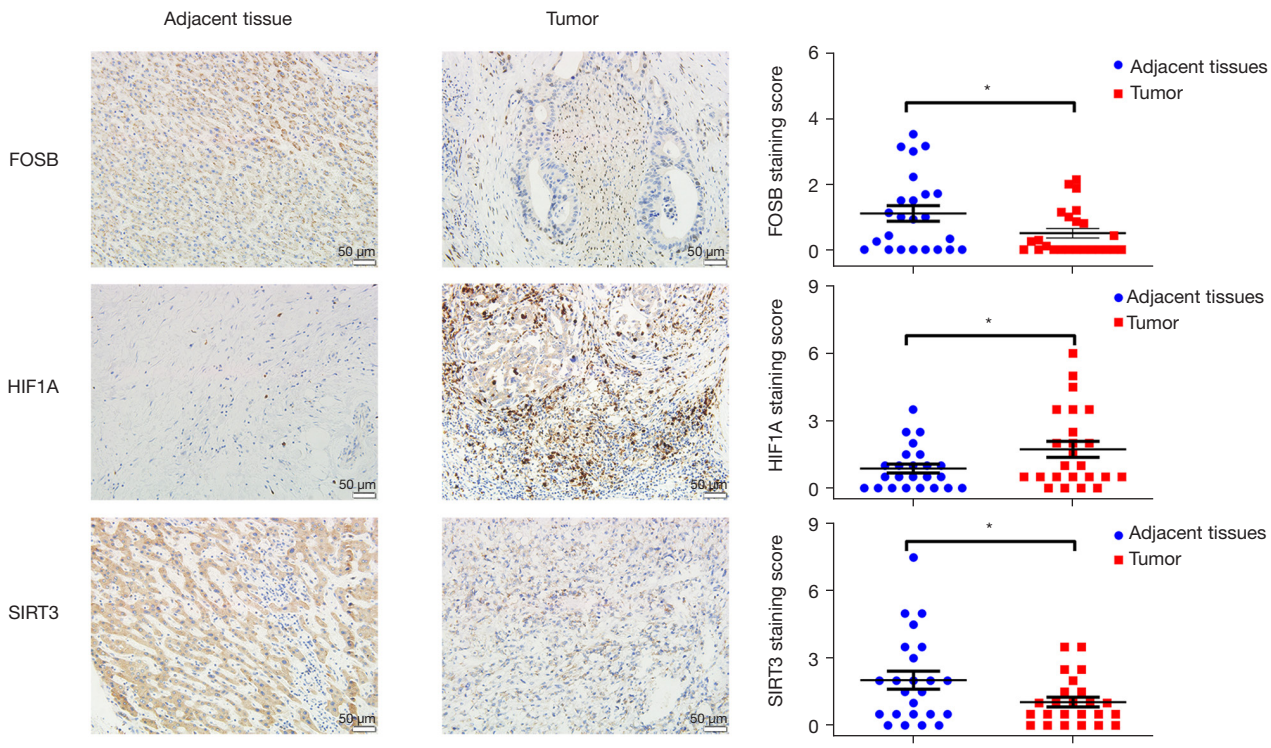

Figure 6 Immunohistochemical picture and expression analysis of *FOSB*, *SIRT3* and *HIF1A* in CCA and adjacent tissues (*, P<0.05). Original magnification, 400-fold. *FOSB*, FBJ murine osteosarcoma viral oncogene homolog B; CCA, cholangiocarcinoma.

thyroid cancer, pancreatic cancer, and so on (48-50), it may also function as a cancer inhibitor in gastric cancer (25,51). Our results show that *FOSB* can inhibit the progression of CCA. However, whether its function is realized by the *SIRT3/HIF1A* axis needs further study. There are some limitations in our study. Bioinformatics analysis and IHC are only preliminary explorations, and only a simple trend can be observed. Specific correlation analysis, protein level validation, cellular experiments, and animal experiments are still lacking.

In general, we speculate that *FOSB* may be a potential prognostic and therapeutic target.

Conclusions

FOSB and the *SIRT3/HIF1A* axis have similar expression trends in CCA, and both are closely related to metabolism, which is associated with poor prognosis in CCA.

Acknowledgments

We thank Dr. Zhangwei Xu and Dr. Weiping Zhang from the Department of Gastroenterology of the First Affiliated Hospital of Anhui Medical University for offering their assistance. Dr. Xu provided help in verifying the interaction between *SIRT3* and *HIF1A*, and Dr. Zhang provided suggestions for the whole research design idea.

Funding: This project was supported by grants from the National Natural Science Foundation of China (No. 61976007) and the Youth Program of Natural Science Foundation of Anhui Province (No. 2008085QH415).

Footnote

Reporting Checklist: The authors have completed the REMARK reporting checklist. Available at https://tcr.amegroups.com/article/view/10.21037/tcr-23-829/rc

Data Sharing Statement: Available at https://tcr.amegroups.com/article/view/10.21037/tcr-23-829/dss

Peer Review File: Available at https://tcr.amegroups.com/article/view/10.21037/tcr-23-829/prf

Conflicts of Interest: All authors have completed the ICMJE uniform disclosure form (available at https://tcr.amegroups.com/article/view/10.21037/tcr-23-829/coif). The authors have no conflicts of interest to declare.

Ethical Statement: The authors are accountable for all aspects of the work in ensuring that questions related to the accuracy or integrity of any part of the work are appropriately investigated and resolved. The study was conducted in accordance with the Declaration of Helsinki (as revised in 2013). The study was approved by the ethics committee of Anhui Medical University (No. 20190199) and informed consent was provided by all patients.

References

1. Bertuccio P, Malvezzi M, Carioli G, et al. Global trends in mortality from intrahepatic and extrahepatic cholangiocarcinoma. J Hepatol 2019;71:104-14.
2. Khan SA, Tavolari S, Brandi G. Cholangiocarcinoma: Epidemiology and risk factors. Liver Int 2019;39 Suppl 1:19-31.
3. Rodrigues PM, Olaizola P, Paiva NA, et al. Pathogenesis of Cholangiocarcinoma. Annu Rev Pathol 2021;16:433-63.
4. Rizvi S, Khan SA, Hallemeier CL, et al. Cholangiocarcinoma - evolving concepts and therapeutic strategies. Nat Rev Clin Oncol 2018;15:95-111.
5. Sirica AE, Gores GJ, Groopman JD, et al. Intrahepatic Cholangiocarcinoma: Continuing Challenges and Translational Advances. Hepatology 2019;69:1803-15.
6. Izquierdo-Sanchez L, Lamarca A, La Casta A, et al. Cholangiocarcinoma landscape in Europe: Diagnostic, prognostic and therapeutic insights from the ENSCCA Registry. J Hepatol 2022;76:1109-21.
7. Brindley PJ, Bachini M, Ilyas SI, et al. Cholangiocarcinoma. Nat Rev Dis Primers 2021;7:65.
8. Banales JM, Marin JJG, Lamarca A, et al. Cholangiocarcinoma 2020: the next horizon in mechanisms and management. Nat Rev Gastroenterol Hepatol 2020;17:557-88.
9. Macias RIR, Cardinale V, Kendall TJ, et al. Clinical relevance of biomarkers in cholangiocarcinoma: critical revision and future directions. Gut 2022;71:1669-83.
10. Raggi C, Taddei ML, Rae C, et al. Metabolic

reprogramming in cholangiocarcinoma. J Hepatol 2022;77:849-64.
11. Ruiz de Gauna M, Biancaniello F, González-Romero F, et al. Cholangiocarcinoma progression depends on the uptake and metabolization of extracellular lipids. Hepatology 2022;76:1617-33.
12. Martínez-Reyes I, Chandel NS. Cancer metabolism: looking forward. Nat Rev Cancer 2021;21:669-80.
13. Chen MH, Yen CC, Cheng CT, et al. Identification of SPHK1 as a therapeutic target and marker of poor prognosis in cholangiocarcinoma. Oncotarget 2015;6:23594-608.
14. Pyne NJ, El Buri A, Adams DR, et al. Sphingosine 1-phosphate and cancer. Adv Biol Regul 2018;68:97-106.
15. Wu T. Cyclooxygenase-2 and prostaglandin signaling in cholangiocarcinoma. Biochim Biophys Acta 2005;1755:135-50.
16. Pastore M, Lori G, Gentilini A, et al. Multifaceted Aspects of Metabolic Plasticity in Human Cholangiocarcinoma: An Overview of Current Perspectives. Cells 2020;9:596.
17. Xu L, Li Y, Zhou L, et al. SIRT3 elicited an anti-Warburg effect through HIF1α/PDK1/PDHA1 to inhibit cholangiocarcinoma tumorigenesis. Cancer Med 2019;8:2380-91.
18. Milde-Langosch K. The Fos family of transcription factors and their role in tumourigenesis. Eur J Cancer 2005;41:2449-61.
19. Park J, Eisenbarth D, Choi W, et al. YAP and AP-1 Cooperate to Initiate Pancreatic Cancer Development from Ductal Cells in Mice. Cancer Res 2020;80:4768-79.
20. Feldker N, Ferrazzi F, Schuhwerk H, et al. Genome-wide cooperation of EMT transcription factor ZEB1 with YAP and AP-1 in breast cancer. EMBO J 2020;39:e103209.
21. Koo JH, Plouffe SW, Meng Z, et al. Induction of AP-1 by YAP/TAZ contributes to cell proliferation and organ growth. Genes Dev 2020;34:72-86.
22. He L, Pratt H, Gao M, et al. YAP and TAZ are transcriptional co-activators of AP-1 proteins and STAT3 during breast cellular transformation. Elife 2021;10:e67312.
23. Thompson BJ. YAP/TAZ: Drivers of Tumor Growth, Metastasis, and Resistance to Therapy. Bioessays 2020;42:e1900162.
24. Guo S, Li J, Huang Z, et al. The CBS-H(2)S axis promotes liver metastasis of colon cancer by upregulating VEGF through AP-1 activation. Br J Cancer 2022;126:1055-66.
25. Tang C, Jiang Y, Shao W, et al. Abnormal expression of FOSB correlates with tumor progression and poor survival in patients with gastric cancer. Int J Oncol 2016;49:1489-96.
26. Luan SH, Ma YQ, Yang JJ, et al. [The Prognostic Value of FOSB Gene in Acute Myeloid Leukemia]. Zhongguo Shi Yan Xue Ye Xue Za Zhi 2022;30:1063-70.
27. Zhou J, Xiong W, Wang Y, et al. Protein Function Prediction Based on PPI Networks: Network Reconstruction vs Edge Enrichment. Front Genet 2021;12:758131.
28. Győrffy B, Lanczky A, Eklund AC, et al. An online survival analysis tool to rapidly assess the effect of 22,277 genes on breast cancer prognosis using microarray data of 1,809 patients. Breast Cancer Res Treat 2010;123:725-31.
29. Tang Z, Kang B, Li C, et al. GEPIA2: an enhanced web server for large-scale expression profiling and interactive analysis. Nucleic Acids Res 2019;47:W556-60.
30. Ru B, Wong CN, Tong Y, et al. TISIDB: an integrated repository portal for tumor-immune system interactions. Bioinformatics 2019;35:4200-2.
31. Li T, Fu J, Zeng Z, et al. TIMER2.0 for analysis of tumor-infiltrating immune cells. Nucleic Acids Res 2020;48:W509-14.
32. Zhao M, Wang S, Zuo A, et al. HIF-1α/JMJD1A signaling regulates inflammation and oxidative stress following hyperglycemia and hypoxia-induced vascular cell injury. Cell Mol Biol Lett 2021;26:40.
33. Hu B, Yu M, Ma X, et al. IFNα Potentiates Anti-PD-1 Efficacy by Remodeling Glucose Metabolism in the Hepatocellular Carcinoma Microenvironment. Cancer Discov 2022;12:1718-41.
34. Mao X, Xu J, Wang W, et al. Crosstalk between cancer-associated fibroblasts and immune cells in the tumor microenvironment: new findings and future perspectives. Mol Cancer 2021;20:131.
35. Özdemir BC, Pentcheva-Hoang T, Carstens JL, et al. Depletion of carcinoma-associated fibroblasts and fibrosis induces immunosuppression and accelerates pancreas cancer with reduced survival. Cancer Cell 2014;25:719-34.
36. Laklai H, Miroshnikova YA, Pickup MW, et al. Genotype tunes pancreatic ductal adenocarcinoma tissue tension to induce matricellular fibrosis and tumor progression. Nat Med 2016;22:497-505.
37. Hosein AN, Brekken RA, Maitra A. Pancreatic cancer stroma: an update on therapeutic targeting strategies. Nat Rev Gastroenterol Hepatol 2020;17:487-505.
38. Fingas CD, Bronk SF, Werneburg NW, et al. Myofibroblast-derived PDGF-BB promotes Hedgehog survival signaling in cholangiocarcinoma cells. Hepatology

2011;54:2076-88.
39. Lin Y, Cai Q, Chen Y, et al. CAFs shape myeloid-derived suppressor cells to promote stemness of intrahepatic cholangiocarcinoma through 5-lipoxygenase. Hepatology 2022;75:28-42.
40. Mertens JC, Fingas CD, Christensen JD, et al. Therapeutic effects of deleting cancer-associated fibroblasts in cholangiocarcinoma. Cancer Res 2013;73:897-907.
41. Thongchot S, Vidoni C, Ferraresi A, et al. Cancer-Associated Fibroblast-Derived IL-6 Determines Unfavorable Prognosis in Cholangiocarcinoma by Affecting Autophagy-Associated Chemoresponse. Cancers (Basel) 2021;13:2134.
42. Bell EL, Emerling BM, Ricoult SJ, et al. SirT3 suppresses hypoxia inducible factor 1α and tumor growth by inhibiting mitochondrial ROS production. Oncogene 2011;30:2986-96.
43. Gong Y, Tang N, Liu P, et al. Newcastle disease virus degrades SIRT3 via PINK1-PRKN-dependent mitophagy to reprogram energy metabolism in infected cells. Autophagy 2022;18:1503-21.
44. Dong D, Dong Y, Fu J, et al. Bcl2 inhibitor ABT737 reverses the Warburg effect via the Sirt3-HIF1α axis to promote oxidative stress-induced apoptosis in ovarian cancer cells. Life Sci 2020;255:117846.
45. Chazenbalk G, Chen YH, Heneidi S, et al. Abnormal expression of genes involved in inflammation, lipid metabolism, and Wnt signaling in the adipose tissue of polycystic ovary syndrome. J Clin Endocrinol Metab 2012;97:E765-70.
46. Yadav S, Kalra N, Ganju L, et al. Activator protein-1 (AP-1): a bridge between life and death in lung epithelial (A549) cells under hypoxia. Mol Cell Biochem 2017;436:99-110.
47. Kotla S, Singh NK, Kirchhofer D, et al. Heterodimers of the transcriptional factors NFATc3 and FosB mediate tissue factor expression for 15(S)-hydroxyeicosatetraenoic acid-induced monocyte trafficking. J Biol Chem 2017;292:14885-901.
48. Barrett CS, Millena AC, Khan SA. TGF-β Effects on Prostate Cancer Cell Migration and Invasion Require FosB. Prostate 2017;77:72-81.
49. Du J, Fu L, Ji F, et al. FosB recruits KAT5 to potentiate the growth and metastasis of papillary thyroid cancer in a DPP4-dependent manner. Life Sci 2020;259:118374.
50. Kim JH, Lee JY, Lee KT, et al. RGS16 and FosB underexpressed in pancreatic cancer with lymph node metastasis promote tumor progression. Tumour Biol 2010;31:541-8.
51. Yu Y, Li H, Wu C, et al. Circ_0021087 acts as a miR-184 sponge and represses gastric cancer progression by adsorbing miR-184 and elevating FOSB expression. Eur J Clin Invest 2021;51:e13605.

Cite this article as: Zhao Y, Tang H, Kuai Y, Xu J, Sun B, Li Y. Identification of the function of *FOSB* in cholangiocarcinoma using bioinformatics analysis. Transl Cancer Res 2023;12(12):3629-3640. doi: 10.21037/tcr-23-829

